Minimum acceleration criterion with constraints implies bang-bang control as an underlying principle for optimal trajectories of arm reaching movements

Shay Ben-Itzhak[1] and Amir Karniel[2]

1. Department of Electrical Engineering, Technion – Israel Institute of Technology, Haifa, Israel
2. Department of Biomedical Engineering, Ben-Gurion University of the Negev, Beer-Sheva, Israel

Correspondence to akarniel@bgu.ac.il

Ben-Itzhak S. and Karniel A. (in press) Minimum acceleration criterion with constraints implies bang-bang control as an underlying principle for optimal trajectories of arm reaching movements. ***Neural Computation***, accepted for publication, April 20, 2007.

Abstract

Rapid arm reaching movements serve as an excellent test bed for any theory about trajectory formation. How are these movements planned? A minimum acceleration criterion has been examined in the past and the solution obtained, based on the Euler-Poisson equation, failed to predict that the hand would begin and end the movement at rest (i.e. with zero acceleration). Therefore this criterion was rejected in favor of the minimum jerk which was proved to be successful in describing many features of human movements. This paper follows an alternative approach, and solves the minimum acceleration problem with constraints using Pontryagin's minimum principle. We use the minimum principle to obtain minimum acceleration trajectories and use the jerk as a control signal. In order to find a solution that does not include non-physiological impulse functions, constraints on the maximum and minimum jerk values are assumed. The analytical solution provides a three phase piecewise constant jerk signal (bang-bang control) where the magnitude of the jerk and the two switching times depend on the magnitude of the maximum and minimum available jerk values. This result fits the observed trajectories of reaching movements and takes into account both the extrinsic coordinates and the muscle limitations in a single framework. The minimum acceleration with constraints principle is discussed as a unifying approach for many observations about the neural control of movements.

1. Introduction

The fast reaching movement is an elementary motor task mastered by humans and primates from early age and is thought to be a primitive for more complex tasks (Morasso 1981; Hogan 1984; Gomi and Kawato 1996; Karniel and Inbar 1997; Smith et al. 2000; Shadmehr and Wise 2005). Rapid reaching movements are also called ballistic movements, since delays in the nervous system and in muscle activation prohibit the effective use of feedback in the first part of the movement, a phenomenon that was fruitfully employed to study the planning of movement and the capability of the brain to expect external perturbations (Shadmehr and Mussa-Ivaldi 1994; Bhushan and Shadmehr 1999; Karniel and Mussa-Ivaldi 2003; Patton and Mussa-Ivaldi 2004). Due to redundancy in the motor system there are various ways to reach from one point in space to another utilizing different hand or joint trajectories and muscles activations (Bernstein 1967). Experimental studies demonstrate that in typical conditions, point to point reaching movements are made using straight line spatial trajectory and bell-shaped speed profiles (Morasso 1981; Abend et al. 1982). How and why does the brain generate these well-observed invariant profiles?

The first question (the how) has been addressed by various computational models. Some of these models elaborate on the neural aspects of the system (Jordan 1996; Barto et al. 1999) while others focus on the muscle dynamics. Nonlinearities of the muscles and the spinal reflex loop may play a major role in generating the observed smooth bell shaped speed profiles (Karniel and Inbar 1997; Krylow and Rymer 1997; Gribble et al. 1998; Karniel and Inbar 1999). In order to answer the second question (the why) researchers usually assume that the biological system evolved to find optimal solutions and under this approach the question is what is the cost function of the trajectory that is being minimized. A few approaches were proposed to determine this cost functions. One approach is to minimize quantities that depend on the dynamics of the system. In this category one can find minimum energy (Nelson 1983), minimum torque-change (Uno et al. 1989), and minimum isometric muscle torque-change (Kashima and Isurugi 1998). Another approach is to minimize quantities that depend on the kinematics of the system, i.e. displacement and its derivatives in task-space coordinates (or angles and its derivatives in joints coordinates). In this category one can find minimum acceleration, minimum jerk, minimum snap and minimum crackle (Nelson 1983; Flash and Hogan 1985; Stein et al. 1986; Richardson and Flash 2002; Dingwell et al. 2004). A third approach suggests minimizing the errors caused by noise in the nervous system or environmental disturbances, which inserts noise both to the control signal, and to the feedback sensors (Harris and Wolpert 1998).

The first approach considers physical quantities, such as energy and torque, directly. The third approach must refer to these physical quantities indirectly in order to compute the influence of the noise. Both approaches require complex calculations in order to find the optimal trajectory. On the other hand, with the second approach, where only the kinematics is considered, the optimal trajectory can be more easily derived analytically. Beyond this appeal to modelers the second approach emphasize the end point (the hand) as the relevant point for the optimization in contrast to other approaches that consider joint space or muscle space.

Traditionally, solutions to a minimum criterion which involve kinematics quantities were calculated analytically using the Euler-Poisson Equation. Using an n-th order derivative of the hands position as the optimum criterion, the Euler-Poisson equation which is an ordinary differential equation, implies that the optimal trajectory is a ($2n$-1)th order polynomial function of time. The constants can be found by applying the boundary conditions. For example, minimum jerk with $n = 3$, has boundary conditions of zero velocity and zero acceleration at the start and at the end of the movement (Richardson and Flash 2002). Figure 1 depicts the speed profile predicted by this method. The analytical solution of the minimum acceleration criterion (MAC) shows no zero acceleration at the boundaries. This contradicts the observed hand rest in reaching movement before and after the movement – therefore the MAC was rejected (Stein et al. 1986). The minimum jerk criterion (MJC) satisfies displacement, velocity and acceleration boundary conditions, and it became the most widespread criterion among the criterions of the second approach. A substantial body of research has demonstrated that this criterion can be used to explain a wide range of experimental data about human arm movements.(Flash and Sejnowski 2001; Sosnik et al. 2004)

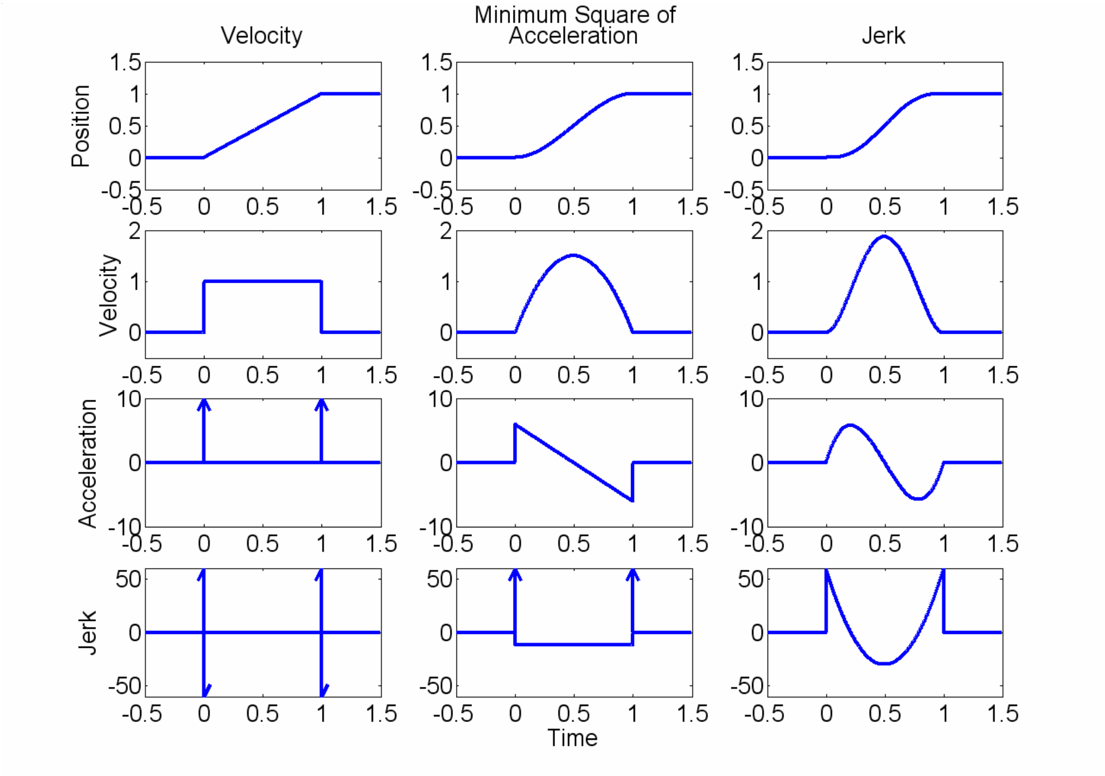

Figure 1. Position, velocity, acceleration and jerk trajectories given by Euler-Poisson equation using different optimality criteria – minimum velocity (left column), minimum acceleration (middle column) and minimum jerk (right column). Units are normalized to the duration (T) and length (L) of the movement, i.e., speed in L/T, acceleration in L/T^2 and Jerk in L/T^3

In this study we propose a remedy to the MAC by adding acceleration boundary conditions and developing an analytical solution instead of changing the optimization criteria. We propose a new approach based on Pontryagin minimum principle (Pontryagin et al. 1962). In order to find a physiologically plausible solution, we also assumed constraints on the maximum and minimum jerk values, so we call our criterion "A Minimum Acceleration Criterion with Constraints" (MACC). The MACC predictions are compared with those of the Minimum Jerk Criterion (MJC), and with experimental results. The derivation and proof of the optimal solution is difficult, in the sense that it requires modern analytical tools such as optimal control theory. However the actual solution is quite simple – only two parameters should be determined in order to realize the optimal solution – and could be easily calculated by the nervous system in real time.

The rest of this paper is organized as follows: In the next section we present the main theorem and analytically derive the trajectory predicted by the MACC. The solution is described rigorously and concisely deferring the details to four appendixes. In section 3 we compare the predictions of the MACC to the predictions of the minimum jerk criterion. In section 4 we compare the predictions of the MACC to experimental results and in section 5 we discuss the advantages and limitations of the MACC hypothesis.

2. Minimum Acceleration Criterion with Constraints (MACC)

We strive to find the movement trajectory of the hand, which begins in a predefined start point and reaches a predefined end point at a predefined time. The beginning and end of the movement are defined by zero velocity and acceleration. Among all possible trajectories we wish to find the trajectory which achieves a minimum mean squared acceleration. In order to find a general solution we employ tools from optimal control theory and formulate our task as a general optimal control problem, for extended background on this theory the reader is referred to one of the textbooks on optimal control theory (Kirk 1970; Macki and Strauss 1982; Lewis 1992).

In this formulation, a state vector, a control signal, and a cost function should be defined, and boundary conditions for the state vector, and an admissible control (i.e. limitations on the control signal) should be stated. The state vector is defined as the position of the hand, and its first and second derivatives (velocity and acceleration respectively). The control signal is defined as the end point jerk (third derivative). The cost function is described as the integral of the squared acceleration over the whole movement. The limitations on the jerk are considered to be isomorphic (i.e. the maximum available jerk can not exceed a certain amount which is the same for each direction).

Hand reaching movements are performed in the physical world in one two or three dimensions however the theorem that we present could be also applied to joint angles or to other problems and therefore we present the problem and the theorem in the general case. Then we first show that the solution lies along a straight line (Lemma 1) and then present Lemma 2 which is the one dimension version of the theorem and could be used for most applications. Therefore the reader who is not interested in the general case and detailed proof may move to Lemma 2, observe Figure 3, skip the proofs and move to Section 3 and 4 which address only the particular solution presented in Lemma 2 and Figure 3.

The Problem

In n-dimensional space, the state vector $\underline{\mathbf{X}}$ is defined as follows:

$$\underline{\boldsymbol{x}}(t)=\begin{bmatrix}x_1(t)\\ \vdots \\ x_n(t)\end{bmatrix};\qquad \underline{\dot{\boldsymbol{x}}}(t)=\begin{bmatrix}\dot{x}_1(t)\\ \vdots \\ \dot{x}_n(t)\end{bmatrix};\qquad \underline{\ddot{\boldsymbol{x}}}(t)=\begin{bmatrix}\ddot{x}_1(t)\\ \vdots \\ \ddot{x}_n(t)\end{bmatrix};$$

$$\underline{\mathbf{X}}=\begin{bmatrix}\underline{\boldsymbol{x}}(t)\\ \underline{\dot{\boldsymbol{x}}}(t)\\ \underline{\ddot{\boldsymbol{x}}}(t)\end{bmatrix}\quad;\qquad \underline{\boldsymbol{u}}(t)=\begin{bmatrix}\dddot{x}_1(t)\\ \vdots \\ \dddot{x}_n(t)\end{bmatrix}$$

the system is described by

$$\underline{\dot{\mathbf{X}}}(t)=\begin{bmatrix}\underline{\dot{\boldsymbol{x}}}(t)\\ \underline{\ddot{\boldsymbol{x}}}(t)\\ \underline{\boldsymbol{u}}(t)\end{bmatrix}=\underline{\boldsymbol{f}}\left(\underline{\mathbf{X}},\underline{\boldsymbol{u}}\right);$$

the boundary conditions are:

$$\underline{\boldsymbol{x}}(0)=\begin{bmatrix}x_{1_0}\\ \vdots \\ x_{n_0}\end{bmatrix}\quad;\qquad \underline{\boldsymbol{x}}(T)=\begin{bmatrix}x_{1_f}\\ \vdots \\ x_{n_f}\end{bmatrix}$$

$$where\ \sum_{i=1}^{n}\left(x_{i_f}-x_{i_0}\right)^2=L^2\qquad;$$

$$\underline{\dot{\boldsymbol{x}}}(0)=\underline{\ddot{\boldsymbol{x}}}(0)=\underline{\dot{\boldsymbol{x}}}(T)=\underline{\ddot{\boldsymbol{x}}}(T)=\underline{\mathbf{0}}$$

and the cost function is:

$$J(\underline{\mathbf{X}},\underline{\boldsymbol{u}})=\tfrac{1}{2}\int_0^T\sum_{i=1}^{n}\dddot{x}_i^{\,2}(t)\,dt=\tfrac{1}{2}\int_0^T f_0\left(\underline{\mathbf{X}}(t),\underline{\boldsymbol{u}}(t)\right)dt$$

Here vectors are written in bold and underlined, T is the movement duration, and L is the movement length, $L\geq 0, T\geq 0$.

The constraint on the jerk value is defined by: $\sum_{i=1}^{n}u_i^{\,2}(t)\leq u_m$

Then, among all the trajectories that satisfy these conditions we searched for the trajectory which minimizes the cost function and obtained the following solution.

Theorem: The solution to the above problem is a straight line, of the following form

$$\underline{\boldsymbol{x}}(t) = r(t)\cdot\left(\underline{\boldsymbol{x}}(T) - \underline{\boldsymbol{x}}(0)\right)$$

where $\underline{\boldsymbol{x}}(0)$ and $\underline{\boldsymbol{x}}(T)$ are the initial point and end point of the movement respectively; and *r*(*t*) is a time dependent function consist of three segments of third order polynomials

$$r(t) = \begin{cases} \frac{1}{6}u_m t^3 & 0 \le t \le t_1 \\ \frac{1}{6}c_0 t^3 - \frac{1}{2}c_1 t^2 + c_2 t + c_3 & t_1 \le t \le t_2 \\ \frac{1}{6}u_m t^3 - \frac{1}{2}u_m T\cdot t^2 + \frac{1}{2}u_m T^2\cdot t - \frac{1}{6}u_m T^3 & t_2 \le t \le T \end{cases}$$

where

$$c_0 = \frac{-24u_m\cdot L}{u_m\cdot T^3 - 24\cdot L + \sqrt{u_m\cdot T^3\left(u_m\cdot T^3 - 24\cdot L\right)}}$$

$$c_1 = \frac{-12u_m\cdot L\cdot T}{u_m\cdot T^3 - 24\cdot L + \sqrt{u_m\cdot T^3\left(u_m\cdot T^3 - 24\cdot L\right)}}$$

$$c_2 = \frac{\left(12\cdot L - u_m\cdot T^3\right)\sqrt{u_m\cdot T} + u_m\cdot T^2\sqrt{u_m\cdot T^3 - 24\cdot L}}{4\sqrt{u_m\cdot T^3 - 24\cdot L}}$$

$$c_3 = \frac{\left(6\cdot L - u_m\cdot T^3\right)\sqrt{u_m\cdot T^3 - 24\cdot L} + \left(u_m\cdot T^3 - 18\cdot L\right)\sqrt{u_m\cdot T^3}}{12\sqrt{u_m\cdot T^3 - 24\cdot L}}$$

and

$$t_1 = \frac{T}{2}\left(1 - \sqrt{\frac{u_m\cdot T^3 - 24\cdot L}{u_m\cdot T^3}}\right)$$

$$t_2 = \frac{T}{2}\left(1 + \sqrt{\frac{u_m\cdot T^3 - 24\cdot L}{u_m\cdot T^3}}\right)$$

Note that the position trajectory lies along the straight line which connects the initial and final hand positions.

Proof:

We first prove that the solution lies along the straight line (Lemma 1) thus reduce the problem to a one dimensional problem. Then we find the solution to this one dimensional case (Lemma 2, which is proved by means of Pontryagin's Theorem and a few additional Lemmas as described below).

Lemma 1:

The solution to the above n-dimensional problem is a straight line path which connects the initial point and end point of the hand movement.

Proof (of Lemma 1):

Without loss of generality (by translating and rotating the axis) we can set the movement to begin at the origin, and to end at $\underline{\boldsymbol{x}}(T)=\begin{bmatrix}L & 0 & \cdots & 0\end{bmatrix}^T$.

Let us assume any initial solution that is not a straight line. Then, the acceleration vector $\underline{\ddot{\boldsymbol{x}}}(t)=\begin{bmatrix}\ddot{x}_1(t) & \cdots & \ddot{x}_n(t)\end{bmatrix}^T$ contains some nonnegative terms in the 2nd ,3rd .. or n-th dimensions at least during part of the time. Now we build a new solution in which $\underline{\ddot{\tilde{\boldsymbol{x}}}}(t)=\begin{bmatrix}\ddot{x}_1(t) & 0 & \cdots & 0\end{bmatrix}^T$. This solution consists of a straight line trajectory. It is clear that in this solution the value of $J\left(\underline{\tilde{\mathbf{X}}},\underline{\tilde{\boldsymbol{u}}}\right)$ is not greater than the value in the initial (not a straight line) solution since,

$$J\left(\underline{\tilde{\mathbf{X}}},\underline{\tilde{\boldsymbol{u}}}\right)=\tfrac{1}{2}\int_0^T\sum_{i=1}^n \ddot{\tilde{x}}_i^{\,2}(t)\,dt=\tfrac{1}{2}\int_0^T \ddot{x}_1^{\,2}(t)\,dt\le\tfrac{1}{2}\int_0^T\sum_{i=1}^n \ddot{x}_i^{\,2}(t)\,dt=J\left(\underline{\mathbf{X}},\underline{\boldsymbol{u}}\right)$$

In addition, the boundary conditions are still satisfied, because in the 2nd, 3rd, .. n-th dimensions:

$$\dot{\tilde{x}}_i(t)=\int_0^t \ddot{\tilde{x}}_i(\tau)d\tau=\int_0^t 0\,d\tau=0 \quad i=2,3,..,n$$

$$\tilde{x}_i(t)=\int_0^t \dot{\tilde{x}}_i(\tau)d\tau=\int_0^t 0\,d\tau=0 \quad i=2,3,..,n$$

and in the 1st dimension the straight line solution is the same as the curved trajectory solution:

$$\dot{\tilde{x}}_1(T)=\int_0^T \ddot{\tilde{x}}_1(\tau)\,d\tau=\int_0^T \ddot{x}_1(\tau)\,d\tau=0$$

$$\tilde{x}_1(T)=\int_0^T \dot{\tilde{x}}_1(\tau)\,d\tau=\int_0^T \dot{x}_1(\tau)\,d\tau=L$$

The jerk maximum value constraint is also satisfied because

$$\tilde{\boldsymbol{u}}(t)=\begin{bmatrix}\dddot{\tilde{x}}_1(t)\\ \vdots \\ \dddot{\tilde{x}}_n(t)\end{bmatrix}=\begin{bmatrix}u_1(t)\\ 0\\ \vdots\\ 0\end{bmatrix}$$

$$\sum_{i=1}^n \tilde{u}_i^2(t)=u_1^2(t)\le\sum_{i=1}^n u_i^2(t)\le u_m$$

Therefore for every curved trajectory we can find a straight line trajectory that satisfies all the boundary conditions and the maximum jerk value constraint, with a value function that is not greater than that of the curved trajectory solution. This straight line goes along the path from initial point to end point of the movement.

Q.E.D (End of proof of Lemma 1)

In Lemma 1 we have reduced the problem to a one-dimensional problem by showing that the trajectory lies on a straight line. Now we find the solution to the one-dimensional case, where the initial point of the movement is given on the origin.

Lemma 2: From all the one dimensional continuous and differentiable trajectories $x(t)$ with first and second continuous and differentiable derivatives, and bounded third derivative $-u_{m_1} \le \dddot{x}(t) \le u_{m_2}$, ($u_{m_1}, u_{m_2} > 0$) which satisfy the boundary conditions $x(0) = \dot{x}(0) = \ddot{x}(0) = \dot{x}(T) = \ddot{x}(T) = 0,\ x(T) = L$, the trajectory that minimizes the cost function $J = \frac{1}{2}\int_0^T \dddot{x}(t)^2\, dt$ is a function consist of three segments of third order polynomials:

$$x(t) = \begin{cases} \frac{1}{6} u_{m_2} t^3 & 0 \le t \le t_1 \\ \frac{1}{6} c_0 t^3 - \frac{1}{2} c_1 t^2 + c_2 t + c_3 & t_1 \le t \le t_2 \\ \frac{1}{6} u_{m_2} t^3 - \frac{1}{2} u_{m_2} T \cdot t^2 + \frac{1}{2} u_{m_2} T^2 \cdot t + L - \frac{1}{6} u_{m_2} T^3 & t_2 \le t \le T \end{cases}$$

Where the coefficients of the polynomial in the intermediate segment are

$$c_0 = \frac{-24 u_{\mathrm{m}_2} \cdot L}{u_{\mathrm{m}_2} \cdot T^3 - 24 \cdot L + \sqrt{u_{\mathrm{m}_2} \cdot T^3 \left(u_{\mathrm{m}_2} \cdot T^3 - 24 \cdot L\right)}}$$

$$c_1 = \frac{-12 u_{\mathrm{m}_2} \cdot L \cdot T}{u_{\mathrm{m}_2} \cdot T^3 - 24 \cdot L + \sqrt{u_{\mathrm{m}_2} \cdot T^3 \left(u_{\mathrm{m}_2} \cdot T^3 - 24 \cdot L\right)}}$$

$$c_2 = \frac{\left(12 \cdot L - u_{\mathrm{m}_2} \cdot T^3\right)\sqrt{u_{\mathrm{m}_2} \cdot T} + u_{\mathrm{m}_2} \cdot T^2 \sqrt{u_{\mathrm{m}_2} \cdot T^3 - 24 \cdot L}}{4\sqrt{u_{\mathrm{m}_2} \cdot T^3 - 24 \cdot L}}$$

$$c_3 = \frac{\left(6 \cdot L - u_{\mathrm{m}_2} \cdot T^3\right)\sqrt{u_{\mathrm{m}_2} \cdot T^3 - 24 \cdot L} + \left(u_{\mathrm{m}_2} \cdot T^3 - 18 \cdot L\right)\sqrt{u_{\mathrm{m}_2} \cdot T^3}}{12\sqrt{u_{\mathrm{m}_2} \cdot T^3 - 24 \cdot L}}$$

and the switching times are

$$t_1 = \frac{T}{2}\left(1 - \sqrt{\frac{u_{\mathrm{m}_2} \cdot T^3 - 24 \cdot L}{u_{\mathrm{m}_2} \cdot T^3}}\right)$$

$$t_2 = \frac{T}{2}\left(1 + \sqrt{\frac{u_{\mathrm{m}_2} \cdot T^3 - 24 \cdot L}{u_{\mathrm{m}_2} \cdot T^3}}\right)$$

Note that to keep $0 < t_1 < t_2 < T$ the maximum admissible jerk must satisfy $u_{m_2} > \frac{24 \cdot L}{T^3}$ and since c_0 is the jerk of the intermediate segment, the minimum admissible jerk must satisfy $-u_{m_1} \le c_0$, otherwise there is no solution to the control problem, i.e. the control signal isn't strong enough to bring the hand to the desired final state in the desired time.

Proof (of Lemma 2):

The following proof is the main thrust of this study and it is based on Pontryagin's minimum principle, which specifies a condition that must be obeyed by the optimal solution. The reader is referred to the optimal control literature for a more detailed description of this fundamental principle (Kirk 1970; Macki and Strauss 1982; Lewis 1992). Pontryagin's principle suggests that the optimal control is attained by finding the control signal, $u(t)$, that minimizes the function *H*, which is known in literature as the Hamiltonian. We consider all the possible trajectories and find the optimal solution by mean of contradiction (reductio ad absurdum) as the only solution that satisfies Pontryagin's minimum principle. We first define the state vector and control signal, cite Pontryagin's minimum principle and formulate our problem in the notations of Pontryagin. Then we describe the nature of all possible solutions and narrow the space of possible solution until we reach the only possible solution. In order to simplify the presentation of the proof we beaked this procedure down to three Lemmas and defer the details of their proof to the appendices.

Let us define a state vector, as the one-dimensional displacement, velocity and acceleration of the trajectory; the control signal as the jerk (i.e. third derivative of displacement); and obtain the system dynamics as follows:

$$\mathbf{X} = \begin{bmatrix} x(t) \\ \dot{x}(t) \\ \ddot{x}(t) \end{bmatrix}, \qquad u(t) = \dddot{x}(t), \qquad \dot{\mathbf{X}} = \begin{bmatrix} \dot{x}(t) \\ \ddot{x}(t) \\ u(t) \end{bmatrix} = f(\mathbf{X}, u)$$

Pontryagin's minimum principle (Pontryagin et al. 1962) [1]: Consider the following system:

$$\dot{\mathbf{X}} = f(\mathbf{X}, u)$$

with an admissible control: $\mathbf{u}_{\min} \le \mathbf{u} \le \mathbf{u}_{\max}$, and the constraints: $\mathbf{x}(0) = \mathbf{x}_0 \quad ; \quad \mathbf{x}(t_f) = \mathbf{x}_f$, and consider a cost function $J = \int_0^{t_f} \mathrm{f}_0(\mathbf{x}(t), \mathbf{u}(t), t)\, dt$.

In addition let us define a function *H* of the variables $\mathbf{X}, u, \mathbf{P}, p_0$ (the Hamiltonian):

$$H(\mathbf{X}, u, \mathbf{P}, p_0) = p_0 \mathrm{f}_0 + \mathbf{P}^T f(\mathbf{X}, u)$$

where the parameters vector **P** satisfies:

$$\dot{\mathbf{P}}_i = -\frac{\partial H}{\partial \mathbf{X}_i}$$

---

[1] In this textbook, the principle is described as maximum principle rather then minimum principle. The only difference in this case is that the function $p_0(t)$ is non-positive so the value function achieves its maximum

Now, let **u** be an admissible control, so that the solution $x_{[0,t_f]}$ provides the boundary conditions. In order that **u**(*t*) yield a solution of the given optimal problem with fixed time it is necessary that there exist a nonzero continuous vector function **P**(t) corresponding to the function **u**(*t*) and **X**(*t*) such that:

1. For all $\{t : 0 < t < t_f\}$, the function *H* of the variable **u** attains its minimum at the point **u** = **u**(*t*).
2. The function $p_0(t)$ is nonnegative (and constant)

[Proof: See (Pontryagin et al. 1962), Chapter 2.]

Following the notation of Pontryagin's minimum principle, since our cost function is $J = \int_0^{t_f} \mathrm{f}_0\left(\mathbf{x}(t), \mathbf{u}(t), t\right) dt = \frac{1}{2}\int_0^1 \ddot{x}(t)^2 dt$, we can write the Hamiltonian as follows:

$$H(u) = \tfrac{1}{2} p_0 \ddot{x}^2 + p_1 \dot{x} + p_2 \ddot{x} + p_3 u$$

where $p_1(t), p_2(t), p_3(t)$ are continuous, differentiable and bounded in $t \in [0, T]$, and comply with the time differential equations:

$$\begin{aligned} \dot{p}_1(t) &= 0 \\ \dot{p}_2(t) &= -p_1(t) \\ \dot{p}_3(t) &= -p_0 \ddot{x} - p_2(t) \end{aligned}$$

p_0 is a nonnegative constant, and therefore can be considered as 0 or 1 (if $p_0 > 0$, then any value of p_0 only factorizes the function *H* by a constant, so without loss of generality, p_0 can be set to 1).

Pontryagin's minimum principle asserts that the optimal control signal (in our case the jerk) must minimize the Hamiltonian. One should recall that according to our problem definition the control signal is bounded $-u_{m_1} \le u(t) \le u_{m_2}$ and therefore our goal is to find solve the following minimization problem:

$$\dddot{x}(t) = \underset{u \in [-u_{m1}, u_{m2}]}{\arg\min} \; H(u)$$

To minimize the Hamiltonian ($H(u) \triangleq \tfrac{1}{2} p_0 \ddot{x}^2 + p_1 \dot{x} + p_2 \ddot{x} + p_3 u$) the control signal, $u(t)$, must be maximal and with sign opposite to $p_3(t)$. As a result, the control signal depends on the sign of $p_3(t)$, where $p_3(t)$ might change its sign over the time interval. In addition, there might be time intervals in which $p_3(t) = 0$ along the whole interval. In those intervals the control signal does not affect the Hamiltonian directly, and other considerations should be taken in order to find the control signal. Therefore we can divide the time interval into segments, where in each segment $p_3(t)$ is positive, negative or zero. If $p_3(t) \neq 0$ along the segment, the trajectory is called a non-singular trajectory, and the control signal is maximal and with sign opposite to $p_3(t)$. If $p_3(t) = 0$ the trajectory along the segment is called a singular trajectory, and the control signal should be found indirectly. Each time point in which $p_3(t)$ changes its sign or changes from nonzero to zero or vise versa, is called a switch. A general solution can include just a singular trajectory (i.e. $p_3(t) = 0$ all over the interval), just non-singular trajectories (i.e. $p_3(t) \neq 0$ all over the interval, but can change its sign), or a combination of singular and non-singular trajectories (See Figure 2 for demonstration of a combined solution).

To find the optimal solution we show by contradiction that no solution exist in the case of $p_0 = 0$, and that a singular trajectory must exist.

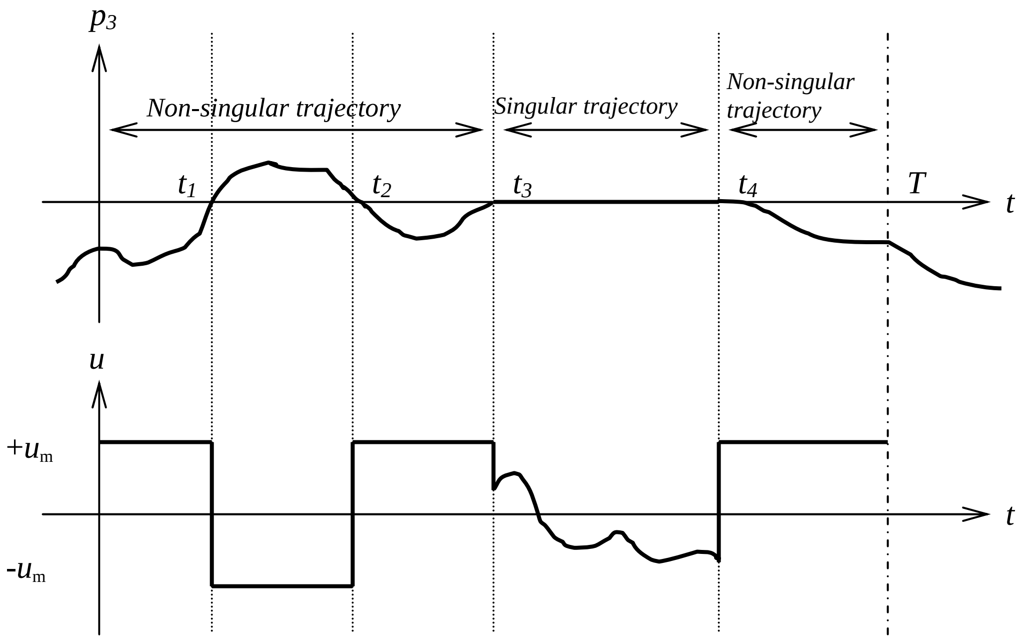

Figure 2: Combined solution which contains singular and non-singular trajectories. If p_3 is non-zero, the control signal exceeds to its maximum or minimum. If p_3 is zero, other considerations should be taken in order to determine the control signal

Lemma 2.1: There is no possible solution to the problem if $p_0 = 0$ (and therefore $p_0 > 0$)

Proof: See Appendix A.

Lemma 2.2: The optimal trajectory must contain an intermediate singular trajectory.

Proof: See Appendix B.

Lemma 2.3: The optimal trajectory must contain only two switches.
Proof: See Appendix C.

From Lemma 2.3 we know that there are only three segments. From Lemma 2.2 the intermediate segment must be singular trajectory therefore the solution consists of one singular trajectory which lies between two non-singular trajectories.
The three trajectories must form an overall continuous trajectory, with continuous first and second derivatives. In addition the overall trajectory must satisfy the boundary conditions. Putting all these constraints together forms a system of 12 equations with 12 unknowns (See section D for details).
In addition, the jerk in the first non-singular trajectory and in the last non-singular trajectory can be positive or negative. Each one of the four possibilities (positive or negative in the first and last non-singular trajectories) gives a different solution, but not all of the solutions are physically acceptable. Solving the equations system four times, with different choices of the jerk sign lead to the conclusion that only in the case of positive jerk either in the first and in the last non-singular trajectories give a solution that satisfies $0 < t_1 < t_2 < T$. All other choices give switching times that are out of the movement time.
Solving the 12 equations system with the right choice of the sign of the jerk, provides the switching times, and the control signal in the singular trajectory [see Appendix D for details]:

$$t_1 = \frac{T}{2}\left(1 - \sqrt{\frac{u_{\mathrm{m}_2} \cdot T^3 - 24 \cdot L}{u_{\mathrm{m}_2} \cdot T^3}}\right)$$

$$t_2 = \frac{T}{2}\left(1 + \sqrt{\frac{u_{\mathrm{m}_2} \cdot T^3 - 24 \cdot L}{u_{\mathrm{m}_2} \cdot T^3}}\right)$$

$$c_0 = \frac{-24 u_{\mathrm{m}_2} \cdot L}{u_{\mathrm{m}_2} \cdot T^3 - 24 \cdot L + \sqrt{u_{\mathrm{m}_2} \cdot T^3 \left(u_{\mathrm{m}_2} \cdot T^3 - 24 \cdot L\right)}}$$

There are two limitations that should be considered in examining this result. As we mentioned before, the switching times should satisfy $0 < t_1 < t_2 < T$ which leads to the requirement that $u_{m_2} > \frac{24 \cdot L}{T^3}$, i.e., if the control signal is not strong enough, the trajectory cannot satisfy the boundary conditions. A second limitation is that the control signal in the singular trajectory should not exceed the boundary $c_0 \geq -u_{m_1}$. This limitation means that if the magnitude of the control signal in the non-singular trajectories is too low, greater jerk must be used in the singular trajectory in order to compensate for the "slowness" of the non-singular trajectories; otherwise the boundary conditions can not be met.

The explicit solution of the optimal trajectory $x(t)$ is thus[see Appendix D for details]:

$$x(t)=\begin{cases} \frac{1}{6}u_{m_2}t^3 & 0\le t\le t_1 \\ \frac{1}{6}c_0t^3-\frac{1}{2}c_1t^2+c_2t+c_3 & t_1\le t\le t_2 \\ \frac{1}{6}u_{m_2}t^3-\frac{1}{2}u_{m_2}T\cdot t^2+\frac{1}{2}u_{m_2}T^2\cdot t+L-\frac{1}{6}u_{m_2}T^3 & t_2\le t\le T \end{cases}$$

where

$$c_0=\frac{-24u_{\mathrm{m}_2}\cdot L}{u_{\mathrm{m}_2}\cdot T^3-24\cdot L+\sqrt{u_{\mathrm{m}_2}\cdot T^3\left(u_{\mathrm{m}_2}\cdot T^3-24\cdot L\right)}}$$

$$c_1=\frac{-12u_{\mathrm{m}_2}\cdot L\cdot T}{u_{\mathrm{m}_2}\cdot T^3-24\cdot L+\sqrt{u_{\mathrm{m}_2}\cdot T^3\left(u_{\mathrm{m}_2}\cdot T^3-24\cdot L\right)}}$$

$$c_2=\frac{\left(12\cdot L-u_{\mathrm{m}_2}\cdot T^3\right)\sqrt{u_{\mathrm{m}_2}\cdot T}+u_{\mathrm{m}_2}\cdot T^2\sqrt{u_{\mathrm{m}_2}\cdot T^3-24\cdot L}}{4\sqrt{u_{\mathrm{m}_2}\cdot T^3-24\cdot L}}$$

$$c_3=\frac{\left(6\cdot L-u_{\mathrm{m}_2}\cdot T^3\right)\sqrt{u_{\mathrm{m}_2}\cdot T^3-24\cdot L}+\left(u_{\mathrm{m}_2}\cdot T^3-18\cdot L\right)\sqrt{u_{\mathrm{m}_2}\cdot T^3}}{12\sqrt{u_{\mathrm{m}_2}\cdot T^3-24\cdot L}}$$

Q.E.D. (End of proof of Theorem 1)

Note that the solution depends only on the maximum admissible jerk. The minimum limit of the jerk influence only the limit of c_0, and the capability (or incapability) of completing the movement. It is also worth noting that the switching times are symmetrically arranged around the middle of the time interval. So learning the solution requires learning only the difference of switching times from middle of the time interval.

Another observation is that in the limiting case of $u_{m_2}\to\infty$, the switching times approach the initial and final times ($t_1\to 0$, $t_2\to T$), and the result reduces to $x(t)=\left(-2\tau^3+3\tau^2\right)\cdot L$, $\tau=\frac{t}{T}$, which is identical to the solution of minimum acceleration criterion that was previously obtained employing Euler-Poisson Equation with no constraints on the control signal (see Figure 1).

3. Minimum Jerk vs. Minimum Acceleration with Constraints

The minimum jerk criterion (MJC) successfully predicts many experimental studies (Flash and Hogan 1985; Sosnik et al. 2004). Therefore any proposed criteria should be able to generate similar predictions under the tested conditions. According to MJC, knowing the boundary conditions of displacement, velocity and acceleration is sufficient for finding the trajectory that satisfies the criterion. The MACC, on the other hand, needs also to know maximum and minimum values of the admissible control signal. These values are important since they affect the shape of the velocity profile and hence affect the agreement of the theoretical solution with experimental results. Low value of maximum admissible control causes the switching times to move toward the middle of the time interval, whereas high value pushes the switching times away from the middle toward the boundaries of the time interval.

Figure 3 depicts some theoretical trajectories for different values of maximum admissible control signal. As one can see, low values create a bell shaped velocity profile, where high values make much more arched shape. As this value approaches infinity, the solution converges to the classical minimum acceleration solution obtained from Euler-Poisson equation.

A salient difference between the two models is the shape of the jerk profile. While the MJC attains a second order polynomial control signal, the MACC obtains a piecewise constant control signal. The maximum value of the jerk according to the MJC is $60\,L/T^3$ (Flash and Hogan 1985; Sosnik et al. 2004) whereas by using MACC the boundary conditions of displacement, velocity and acceleration can be realized with almost half of this value ($32\,L/T^3$).

It is also worthwhile to note that the maximum value of acceleration in the solution of MJC is lower than the maximum values obtained by the MACC. However, the overall mean squared acceleration is lower in the MACC than in the MJC when the maximum jerk is similar.

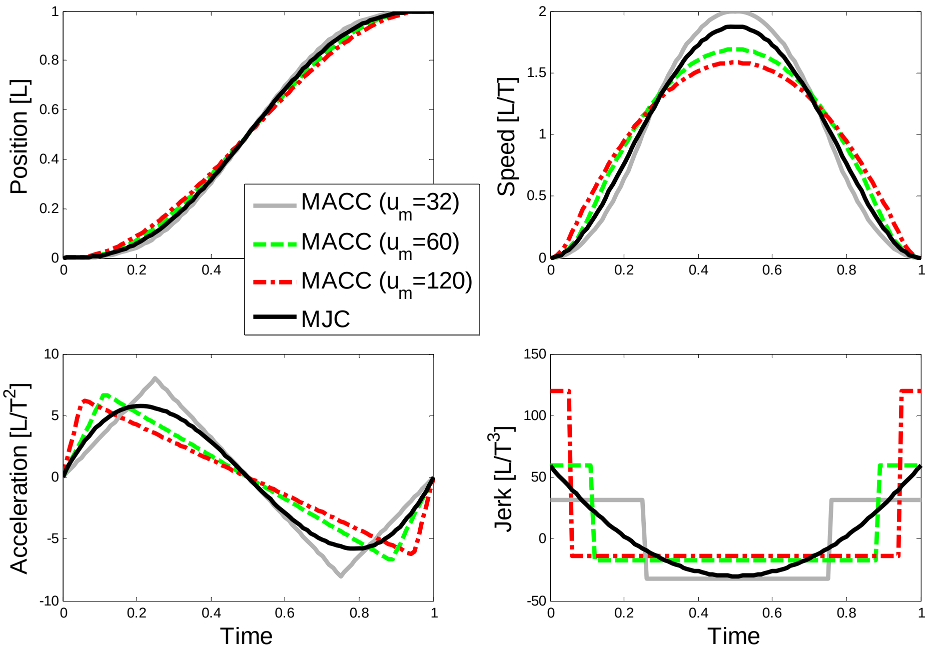

<u>Figure 3.</u> MACC vs. MJC profiles. Displacement, speed, acceleration and jerk trajectories of MACC solution with various jerk limitations. u_m is the maximum admissible jerk. Low admissible jerk (solid gray) produces bell-shaped speed profile. High admissible jerk (dash-dotted) produces arched-shaped speed profile. Medium admissible jerk (dashed) produces intermediate shape. Low admissible jerk speed profile is very close to profile produced by MJC. Units are normalized to the duration (T) and length (L) of the movement, i.e., speed in L/T, acceleration in L/T^2 and Jerk in L/T^3

4. Fitting to experimental results

In this section we compare the theoretical prediction of the MACC hypothesis to human reaching movements obtained in previous studies (Karniel and Mussa-Ivaldi 2002; Karniel and Mussa-Ivaldi 2003).

<u>4.1 The experiment</u>

We present a brief description of the experiment and refer the reader to (Karniel and Mussa-Ivaldi 2002) for further details.

Five subjects participated in the experiment. Seated subjects held the handle of a two degrees of freedom robotic manipulandum and looked at a screen that displayed the location of the hand and the location of the target. The movements were performed in the horizontal plane.

Subjects were asked to execute fast reaching movements to target displayed on the screen. A small round cursor represented the position of the hand and a rectangular one represented the target. As soon as the cursor reached the target, the target either exploded (i.e., become gradually bigger over a period of 200 milliseconds) or changed color instructing the subject to move faster or slower in order to achieve movement duration of approximately one-third of a second (±50 milliseconds). The experiments included three possible targets, which allowed six possible movements of 10 cm (Figure 4). Although the original experiments involved perturbing forces applied to the subjects movements, here we only analyze trials from blocks in which no forces were applied. For more details see (Karniel and Mussa-Ivaldi 2002).

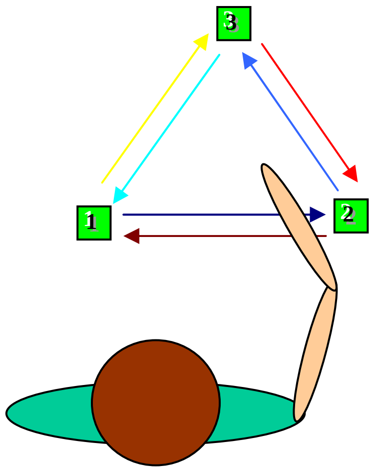

Figure 4: Experimental setup. One of three targets appeared on a screen at each moment triggering one of six possible movements of 10 cm.

4.2 Data analysis

To analyze the raw data, the starting point and the stopping point should be found for each movement. This was done by examining the curvature of the position trajectory, and the acceleration zero crossing. Before the initiation of the movement the acceleration may be positive or negative and the curvature could assume large values, however once the movement starts the acceleration is positive and the movement becomes roughly straight. Therefore we marked the starting at the first time where both conditions were met and hold until maximum velocity is obtained, specifically (i) the acceleration was no longer negative and (ii) the curvature was less then 0.2 radians. The second condition was chosen by trial and error and was aimed to insure a straight line with a reasonable tolerance. In order to avoid feedback effects in the last part of the movement, only the first half of the movement is being analyzed. Since the duration of the movement depends on corrective movements that are not part of our model, we considered only the data at the beginning of the movement up to the point of maximum velocity. The time where the maximum velocity has been reached is considered as the middle of the movement duration, thus the movement overall duration is considered as twice the time to reach the maximum velocity. Figure 5 shows typical movements' velocity, acceleration and curvature profiles and the starting and stopping points.

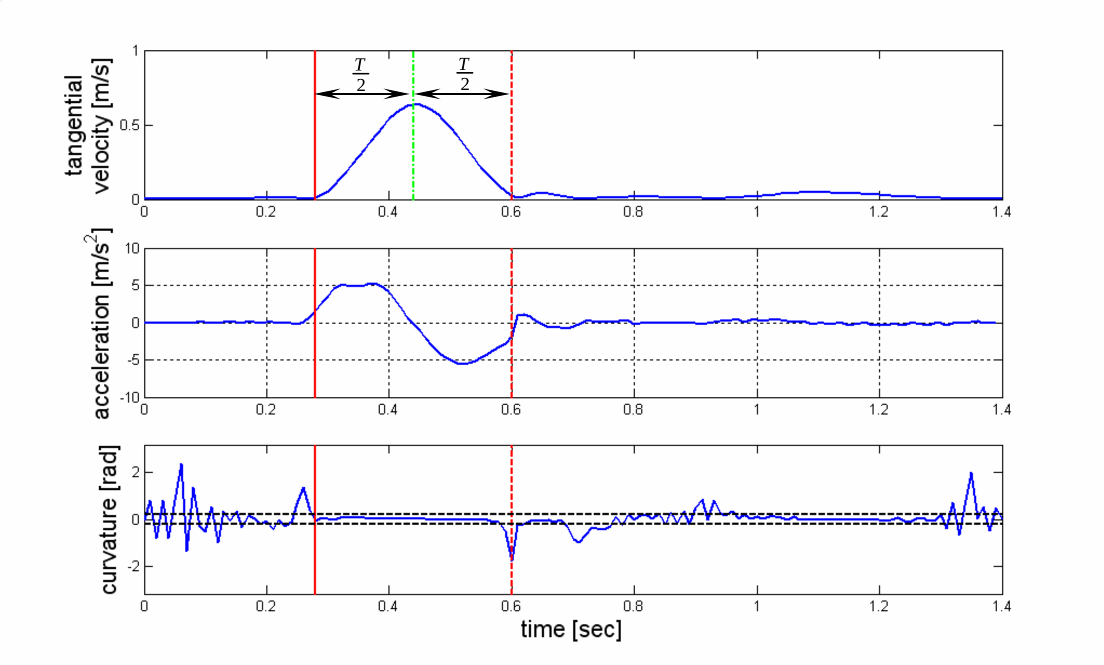

Figure 5: Tangential velocity profile, acceleration profile, and curvature of typical trajectory. Movement starts where both acceleration is positive and curvature is greater than 0.2 [rad] (~11.5 [deg]) (left solid bar). Half time is set where the velocity is maximal (dash-dot bar). Trial duration is set to be twice the time to reach maximum velocity (right dashed bar)

The MACC assumes maximum and minimum jerk value, but existence of such constraints and their values is not known. In order to test the MACC we fitted the value of the maximum available jerk (u_{m_2}) to each trial by minimizing the mean squared error (MSE) of tangential velocity profile. The fitting was performed only to the first half of the movement in order to avoid effects of feed-back. Figure 6 shows the fitting to one typical trial. As one can see, the position and velocity profiles of MJC as well as MACC qualitatively match the experimental data. Outliers were considered as trials where the calculated u_{m_2} was less then $27\frac{L}{T^3}$ (in this case $u_{m_1} > 2u_{m_2}$) or greater then $65\frac{L}{T^3}$ (twice the median) and were removed from the data-set used in further analysis (Since movements duration and length vary between directions and subjects, the value of u_{m_2} was normalized by length and time, and was expressed by means of $\frac{L}{T^3}$ units).

After outline removal we were left with 80,85,79,71,77 trials for subjects 1,2,3,4,5 respectively. These trials where used for the data analysis presented in the next subsection.

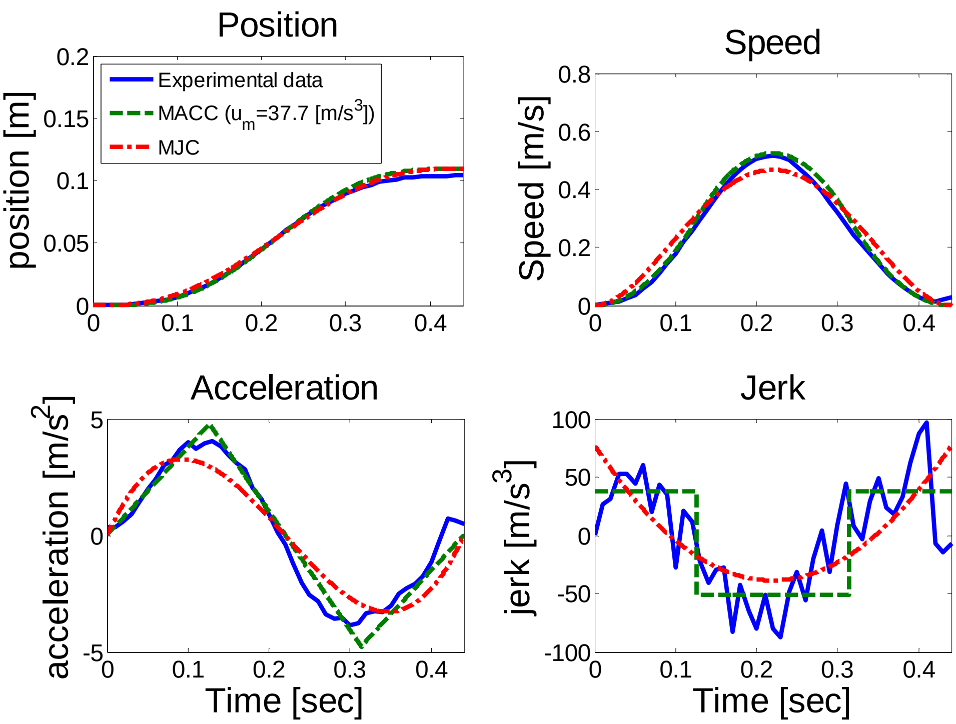

Figure 6. Trajectories of position, velocity, acceleration and jerk. Experimental result (solid), MACC (dashed) and MJC (dash-dotted)

4.3 Comparing the fitting of MJC and MACC to the data

We used two measures to compare the predictions of the MJC and those of the MACC to the data, the expected maximum velocity and the mean error over the trajectory profile (see Figure 7).

From the analytical results of MACC (Lemma 2) one can derive the maximum velocity as a function of u_{m_2}

$$V_{\max} = \tfrac{1}{8}\left(T^2 u_{m_2} - \sqrt{T u_{m_2}\left(T^3 u_{m_2} - 24L\right)}\right)$$

The maximum velocity estimated by MJC is $1.875\tfrac{L}{T}$ (Richardson and Flash 2002).

The difference between MACC estimation and the data was calculated and compared with the difference between MJC estimation and the data. In addition, the sum of squared error in the velocity trajectory between analytic results and experimental data was calculated in every trial (from the initiation of movement up to the point of maximum velocity) for both MJC and MACC. This analysis shows that the MACC can fit the experimental data better than the MJC (Figure 7). The differences between the errors in both measures for each subject were statistically significant ($p<0.01$ using Wilcoxon rank sum test).

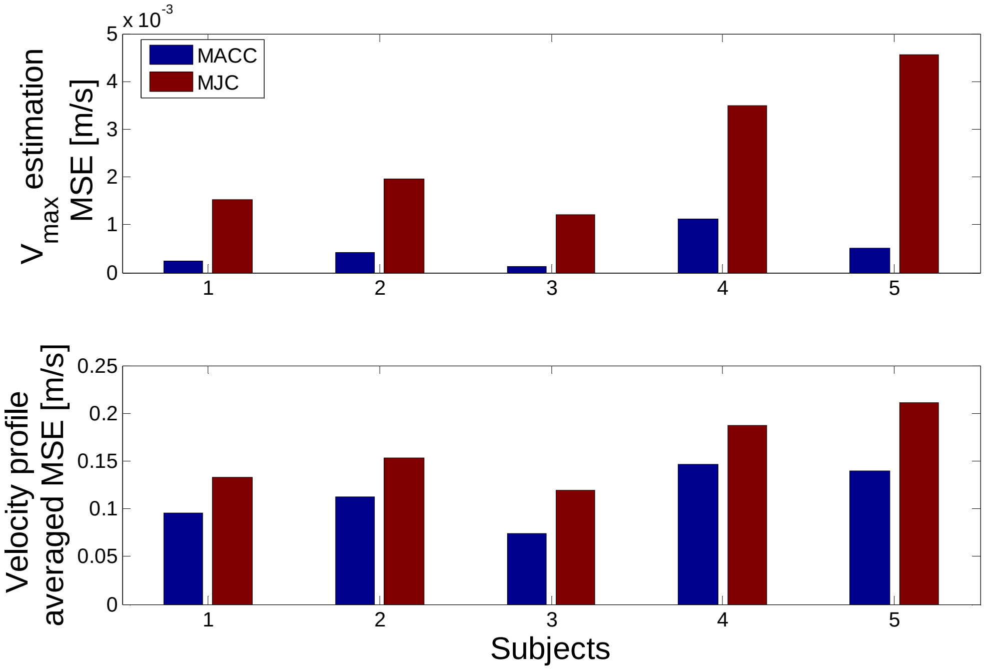

Figure 7. Average of MSE between experimental results and analytic results of MACC and MJC. MSE of Vmax (Top). MSE of velocity profile (Bottom). One can see that the MACC can fit the experimental data better than the MJC. The differences between the errors in both measures for each subject were statistically significant ($p<0.01$)

4.4 The maximum jerk at different movement directions

The maximum Jerk, u_{m_2}, was fitted to each movement.

Although subjects received feedback encouraging them to perform movements of the same duration, the time duration of each trial varied by 12-18 % of median value. The changes in time duration plays an important role in determining the control signal, since the jerk depends on time duration by power of three. Therefore it is difficult to analyze the properties of u_{m_2} that also changes from trial to trial.

Nevertheless, one can still observe differences in the values of the maximum jerk that depend on the direction of the movements. We have calculated the mean of the maximum Jerk for the six directions (Figure 4) for each one of the five subjects (Figure 8). One can see that in four out of five subjects, the maximum jerk value was clearly greater in movements 1→3 and 3→1, movements which do not include shoulder, relative to the other movements that involve shoulder movement, these differences are statistically significant ($p<0.05$ using Wilcoxon rank sum test) only in subjects 1 and 2. This result indicates that the maximum available jerk depends on the muscles and joints properties and therefore the MACC is not a pure extrinsic criterion.

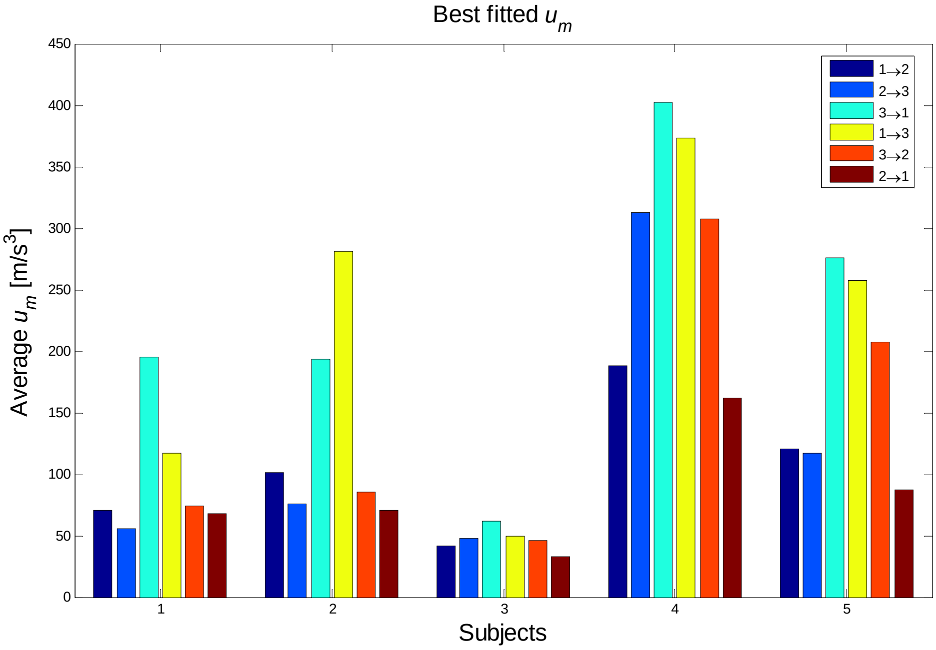

Figure 8: Average of u_m for six directions, in five subjects. One can see that movements from target 1 to target 3 and vise versa have the greatest u_m. It is interesting to note that movements between targets 1 and 3 require much less shoulder movements.

5. Discussion

We present a new criterion for arm trajectory formation, the minimum acceleration with constraints criterion (MACC), analytically derive the expected hand trajectories and compare them to the minimum Jerk criterion as well as to measured hand movements of five subjects.

The solution of the MACC dictates a very simple three phase control signal where the controller should provide only two parameters. The difference of switching times from middle of time interval and the amplitude value of the singular trajectory. This control could be easily learned by trial and error.

The analytical solution assumes an existence of a maximum available jerk value. From our experimental results it is clear that there is no such a unique value, and this value changes from one movement to another. Our physiological interpretation of the bound on the jerk could be related to the neural signal which is integrated before the force is produced and therefore could be similar to jerk, another interpretation is the desire to minimize tear and wear that might increase significantly above certain value of jerk. We already noticed that the maximum value changes with movement type consistently which indicates that the true maximum jerk could be calculated in the joint coordinates. It is not clear that the maximum available jerk value stays constant over one movement and if this is the case the solution presented here should be considered as an approximation of the underlying mechanism that should be further studied. If the admissible jerk control does not stay constant over the whole movement, the analytical solution becomes more complicated, but the policy of finding the optimal control according to the sign of p_3 remains unchanged, in that sense this work could be extended to consider various policies to determine the maximum available jerk at each movement.

We have clearly found that the MACC better fits the experimental data than the MJC for all subjects (Figure 7), nevertheless one should remember that the MACC includes an additional free parameter, the maximum available jerk. As modelers that look for simplicity this could be considered a disadvantage, but considering the physiological interpretation this additional flexibility can indirectly introduce the constraints imposed by the muscles and joints and in that sense the MACC can enjoy the advantageous of the two schools of criteria that concentrate on either the joints or the end-point (see Figure 8). In order to find out whether MACC or MJC are more compliant with experimental data a more accurately measures of acceleration and jerk are required. One of the predictions that could be used to distinguish between the two criteria is the arched-shaped velocity profile for large admissible jerk values. If we assume that the maximum admissible jerk is constant (does not dependent on the length and duration of the movement) then differences in length of movement or in time duration are expected to change the normalized maximum admissible jerk, and consequently the velocity profile. In our experimental data, all the movements were approximately equal in length and time duration. Additional experiments should be done with changes in length and duration, in order to check whether there is a change in velocity profile. Another prediction involves the maximum jerk value which could be rather low in the MACC and in the extreme case almost half of the maximum jerk expected from the MJC, accurate measurements of the maximum jerk under various movement directions and muscle conditions could reveal the potential flexibility of the maximum jerk parameters facilitates by the MACC.
Further study is required in order to thoroughly compare the MACC predictions to the many other alternative criteria partly presented in the introduction, in this work we concentrated on comparison to the minimum jerk criterion due to its simple analytical solution, the other methods require assumptions as to the limb dynamics and/or muscles properties and/or noise distributions and therefore a simple objective comparison is quite difficult. Nevertheless it worth noting that the free parameter inherent in the MACC (the maximum Jerk) provides a bridge to dynamic related criteria since it account to the different profiles observed in different arm configurations and movement directions (see Figure 8) as predicted by muscle and joint related criteria. One prominent prediction of many of the other criteria is a gently curved profile rather than a straight line which is predicted by both MJC and the MACC (see e.g. Harris and Wolpert 1998; Uno et al. 1989). In this respect it is

interesting to note our simplifying assumptions about the value of the maximum jerk being similar in all direction of movements. An interesting direction of future study is generalization of the model to the possibility of different values of the maximum Jerk in different movement directions which may imply non-straight path as observed in some cases, in particular in 3D and at the edge of the workspace.

Dingwell et al. (2004) and recently also (Svinin et al. 2006) tried to predict the trajectory of a hand holding a spring attached to a mass. Following the tradition of using the Euler-Poisson equation, which was used to dismiss the minimum acceleration criterion in favor of the minimum Jerk criterion, Dingwell et al. claim that since the solution of MJC on the mass gives a non-zero acceleration of the hand, a higher derivative of the mass displacement should be taken as the minimum criterion, and a minimum crackle criterion was suggested. According to our approach, using the minimum principle can solve the problem of hand attached to a mass with a spring using MJC, or even using the minimum acceleration, but constraints should be added to the admissible control. Furthermore, if jerk of the hand is considered as the control signal, it is not difficult to show that the control signal is piecewise constant, i.e. a bang-bang control (however further study is required in order to find the number of switches and magnitude of jerk in each segment).

The bang-bang control method was proposed in the past in the context of minimum time which predicts maximum velocity and non-smooth trajectories, predictions which were rightfully criticized as not physiological. In the original minimum acceleration criterion (Figure 1) the acceleration changes abruptly and therefore the predicted trajectories significantly differ from the observed hand movements. It is important to note that here the bang-bang control is in the jerk signal and under the proposed MACC model both position and velocity are smooth and even the acceleration is continuous. The predicted acceleration profile is not smooth, however, abrupt changes in the jerk are also predicted by the MJC and should not be considered not physiological as they represent neural control signal which is being integrated by the musculoskeletal system to generate smooth movement. The neural control signal, measured as firing rate, does not have to be smooth and burst activities are frequently observed in the nervous system, see for example the bistability recently observed in the cerebellum in vivo (Loewenstein et al. 2005)

The MACC predicts bang-bang control and suggests that the brain may control only the transitions rather then sending a continuous command. This approach is consistent with the notion of hierarchy in which the brain sends simple commands that are further translated to movement by the spinal cord muscles and arm dynamics could be traced back to William Harvey[2] who used the analogy of the army to describe the control of movements. More recent studies use the notion of primitives

[2] "Nature sets in motion by signs and watchwords, which are made with little momentum…Just as in the army the soldiers are set in motion by one word as if by a given signal and continue to move until they receive another signal to stop, so the muscles move in order and harmony from established custom." William Harvey (1578-1657)

to describe this notion (Mussa-Ivaldi and Bizzi 2000) in one case even suggesting that the brain minimizes the transitions in its command in order to simplify its efforts for frequently used movements (Karniel et al. 2002). This hypothesis named the minimum transition hypothesis is based on the notion of intermittence control implied by the MACC presented herein.

Woodworth (1988) discussed the distinction between initial adjustment and current control and inspired many modern studies about intermittence control and the notion of generating sub-movements as a result of feedback about error during the movement (Hanneton et al. 1997; Doeringer and Hogan 1998; Novak et al. 2002; Fishbach et al. 2005). Although the MACC do not address the feedback at all, the control strategy predicted by the MACC, of using pulses and steps, perfectly fits with this notion of intermittence control and could serve the basis for a more general view of the motor control system. Such simple motor commands of pulses and steps were used in a few models that describe neural control of movement (Karniel and Inbar 1997; Barto et al. 1999). It is also interesting to note that recent measurements in the cerebellum found clear evidence for an intermittence control strategy (Loewenstein et al. 2005). Whether the brain employs continuous or discrete control strategy is still a fascinating open question. In this study we show that a discrete control strategy could be consistent with the observed smooth movements that were previously explained by mean of continuous control strategies.

An analytical solution for the optimal hand trajectory under MACC was derived. This new criterion predicts simple trajectory of three phase bang-bang control strategy. The bang-bang control strategy is the optimal result of many control problems as described in any textbook on optimal control (Kirk 1970; Macki and Strauss 1982; Lewis 1992) and it is fruitfully used in many systems from missile control to domestic thermostat. Further studies are required to derive predictions for other type of movements, such as reaching through via-points, and to test the predictions of this model by accurately measuring jerk during reaching movements.

All in all it appears that the rumors about the death of the minimum acceleration criterion were premature.

Acknowledgements

We are in debt to many colleagues for numerous discussions about this study; the seeds to this study were planted in a lab meeting with Jim Patton and Sandro Mussa-Ivaldi. In particular we wish to thank Nahum Shimkin, Gideon Inbar, Opher Donchin and Eyal Carmi for their useful comments on earlier versions of this manuscript.

Appendix A

In this appendix we prove lemma 2.1 by contradiction, i.e., we show that there is no possible solution to the problem if $p_0 = 0$.

Assume $p_0 = 0$. Then the Hamiltonian is

$$H = p_1\dot{x} + p_2\ddot{x} + p_3 u$$

and

$$\begin{aligned}
\dot{p}_1(t) &= 0 && \Rightarrow && p_1(t) = c_0 \\
\dot{p}_2(t) &= -p_1(t) && \Rightarrow && p_2(t) = -c_0 t + c_1 \\
\dot{p}_3(t) &= -p_2(t) && \Rightarrow && p_3(t) = \tfrac{1}{2}c_0 t^2 - c_1 t + c_2
\end{aligned}$$

First, let us consider the case where $p_3 \equiv 0$ in a segment (subinterval) $[t_1, t_2] \in [0, T]$ (If $p_3 = 0$ only in a finite number of time points (singular time points), it does not affect the system dynamics). Since $p_1(t), p_2(t), p_3(t)$ do not depend on $x(t)$ or its derivatives, c_0, c_1, c_2 stay constant over the whole time interval $t \in [0, T]$. Because $p_3 \equiv 0$ over a segment $[t_1, t_2] \in [0, T]$, all its derivatives in the segment are also equal to zero:

$$\begin{aligned}
p_3 &= \tfrac{1}{2}c_0 t^2 - c_1 t + c_2 = 0 && \Rightarrow && c_2 = 0 \\
& && && \Uparrow \\
\dot{p}_3 &= -p_2 = c_0 t - c_1 = 0 && \Rightarrow && c_1 = 0 \\
& && && \Uparrow \\
\ddot{p}_3 &= -\dot{p}_2 = p_1 = c_0 = 0 && \Rightarrow && c_0 = 0
\end{aligned}$$

but this leads to the fact that the vector $\mathbf{P} \triangleq \left[p_0, p_1(t), p_2(t), p_3(t)\right]^T$ is identically zero which contradicts the requirement in theorem 1, that $\mathbf{P}$ is a nonzero vector. Therefore there is no segment $[t_1, t_2] \in [0, T]$, in which $p_3 \equiv 0$.

Now, let us consider the case in which $p_3(t) \neq 0$ on any segment in $t \in [0, T]$. The function *H* is linear by *u*, so its minimum is attained at the boundaries of *u*(*t*), that is

$$u(t) = \underset{-u_{m_1} \le u \le u_{m_2}}{\arg\min}\, H(u) = -\operatorname{sgn}\left(p_3(t)\right) \cdot u_{\max},$$

where $u_{\max} = \begin{cases} u_{m_2} & \operatorname{sgn}\left(p_3(t)\right) < 0 \\ u_{m_1} & \operatorname{sgn}\left(p_3(t)\right) > 0 \end{cases}$, and u_{m_1}, u_{m_2} limit the admissible control (jerk of *x*(*t*)).

Since the control signal depends on $p_3(t)$, and $p_3(t)$ might change its sign over the time interval, one can divide the time interval into segments, where in each segment $p_3(t)$ is positive or negative along the whole segment (Figure. 2).

In each segment the solution is of the form:

$$u_i = -\operatorname{sgn}\left(p_3(t)\right)u_{\max}$$
$$\ddot{x} = -\operatorname{sgn}\left(p_3(t)\right)u_{\max}t + {}^i d_0$$
$$\dot{x} = -\tfrac{1}{2}\operatorname{sgn}\left(p_3(t)\right)u_{\max}t^2 + {}^i d_0 t + {}^i d_1$$
$$x = -\tfrac{1}{6}\operatorname{sgn}\left(p_3(t)\right)u_{\max}t^3 + \tfrac{1}{2}\,{}^i d_0 t^2 + {}^i d_1 t + {}^i d_2$$

where i is the index of the segments, and is defined as the number of switches in the control signal before that segment (i.e. i is zero in the first segment). The continuity of $x(t)$ and its first and second derivatives dictates the number of the segments. The boundary conditions, as well as the continuity of $x(t)$ and its first and second derivatives give the following constraints:

$$x(0) = 0 \quad x(T) = L \quad x\left(t_i^-\right) = x\left(t_i^+\right)$$
$$\dot{x}(0) = 0 \quad \dot{x}(T) = 0 \quad \dot{x}\left(t_i^-\right) = \dot{x}\left(t_i^+\right)$$
$$\ddot{x}(0) = 0 \quad \ddot{x}(T) = 0 \quad \ddot{x}\left(t_i^-\right) = \ddot{x}\left(t_i^+\right)$$

where $t_i, i = 1..k$ are the switching times and k is the number of switches. The total number of equations is 6+3k.

The variables to be found are:

$$ {}^i d_0, {}^i d_1, {}^i d_2 \qquad i = 0..k$$
$$ t_i \qquad i = 1..k$$

The total number of variables to be found is 3(k + 1) + k. A general solution might exist only if the total number of variables to be found is equal or greater than the total number of equations. This gives us a lower boundary to the number of switches.

$$6 + 3k \le 3(k+1) + k$$
$$6 + 3k \le 4k + 3$$
$$k \ge 3$$

One can see that the number of switches can not be less then three.

In addition, other constraints should be considered. The Lagrangian multiplier $p_3(t)$ must be zero in all switching times. i.e.

$$p_3(t_i) = \tfrac{1}{2}c_0 t_i^{\,2} - c_1 t_i + c_2 = 0 \qquad i = 1..k$$

But $p_3(t)$ is a second order polynomial, so it can equal zero at most twice, therefore a number of three (or more) switching times is not possible. And we conclude that no possible solution is applicable when $p_0 = 0$.

QED (End of proof of Lemma 2.1)

Appendix B

In this appendix we prove Lemma 2.2, i.e., continue based on the previous appendix and show that the optimal trajectory must contain an intermediate singular trajectory.
The conclusion of Lemma 2.1 is that $p_0 = 1$. The problem is now the same as defined in Appendix A, except that the Hamiltonian is defined as follows:

$$H(u) \triangleq \tfrac{1}{2}\ddot{x}^2 + p_1\dot{x} + p_2\ddot{x} + p_3 u$$

and the third element of the vector $\boldsymbol{P}$ is defined by:

$$\dot{p}_3(t) = -\ddot{x} - p_2(t)$$

By integration, the Lagrangian multipliers are

$$p_1(t) = c_0$$
$$p_2(t) = -c_0 t + c_1$$
$$p_3(t) = -\dot{x} + \tfrac{1}{2}c_0 t^2 - c_1 t + c_2$$

Notice that $p_1(t), p_2(t)$ are independent in *x*(*t*), so c_0, c_1 are constants over the whole interval $t \in [0,T]$. In addition, the first-derivative of *x*(*t*) is continuous and $p_3(t)$ is continuous too, which requires that c_2 is also constant over the whole interval $t \in [0,T]$.

As in Appendix A, one can see that since the control signal depends on the sign of $p_3(t)$, and $p_3(t)$ might change its sign over the time interval, the time interval can be divided into segments, where in each segment $p_3(t)$ is positive, negative or zero along the whole segment (Figure. 2).
Assume (by contradiction) that there are no singular trajectories along the whole interval $t \in [0,T]$. Then the whole interval contains only nonsingular trajectories, and $p_3(t) \neq 0$, which yields $\dddot{x}(t) = -\mathrm{sgn}\, p_3(t) \cdot u_{\max}$, where $u_{\max} = \begin{cases} u_{m2} & \mathrm{sgn}(p_3(t)) < 0 \\ u_{m1} & \mathrm{sgn}(p_3(t)) > 0 \end{cases}$ and u_{m_1}, u_{m_2} limit the admissible control (jerk of *x*(*t*)).

The form of *x*(*t*) and its first and second derivatives in a single segment is as follows:

$$\dddot{x}(t) = -\mathrm{sgn}(p_3(t))u_{\max}$$
$$\ddot{x}(t) = -\mathrm{sgn}(p_3(t))u_{\max}t + {}^i d_0$$
$$\dot{x}(t) = -\tfrac{1}{2}\mathrm{sgn}(p_3(t))u_{\max}t^2 + {}^i d_0 t + {}^i d_1$$
$$x(t) = -\tfrac{1}{6}\mathrm{sgn}(p_3(t))u_{\max}t^3 + \tfrac{1}{2}{}^i d_0 t^2 + {}^i d_1 t + {}^i d_2$$

where i indicates the index of the segment (starting from 0), $\left\{{}^{i}d_j\right\}_{j=0}^{2}$ are constants and $u_{\max}$ as above. The continuity constraints on $x(t)$ and its first and second derivatives dictates the number of segments. Adding the boundary conditions, give the following constraints:

$$x(0)=0 \quad x(T)=L \quad x\left(t_i^-\right)=x\left(t_i^+\right)$$
$$\dot{x}(0)=0 \quad \dot{x}(T)=0 \quad \dot{x}\left(t_i^-\right)=\dot{x}\left(t_i^+\right)$$
$$\ddot{x}(0)=0 \quad \ddot{x}(T)=0 \quad \ddot{x}\left(t_i^-\right)=\ddot{x}\left(t_i^+\right)$$

where $t_i, i=1..k$ are the switching times and k is the number of switches. The total number of equations equals 6+3k.

The variables to be found are:

$$ {}^{i}d_0, {}^{i}d_1, {}^{i}d_2 \qquad i=0..k$$
$$ t_i \qquad i=1..k$$

The total number of variables to be found is 3(k + 1) + k. A general solution might exist only if the total number of variables to be found is equal or greater than the total number of equations. This gives us a lower boundary to the number of switches.

$$6+3k \le 3(k+1)+k$$
$$6+3k \le 4k+3$$
$$k \ge 3$$

One can see that the number of switches can not be less then three, so the number of segments in the total interval can not be less then four.

In addition, other constraints should be considered. The Lagrangian multiplier $p_3(t)$ must be zero in all switching times. i.e.

$$p_3(t_i)=\tfrac{1}{2}\left(c_0+\operatorname{sgn}\left(p_3\left(t_i^-\right)\right)\cdot u_{\max}\right)t_i^2-\left(c_1+{}^{i-1}d_0\right)t_i+\left(c_2-{}^{i-1}d_1\right)=0 \qquad i=1..k$$

Some of the ${}^{i}d_j$ variables were found by the continuity and boundary constraints. The number of yet undetermined variables equals to the difference between the number of variables $(4k+3)$ and the number of equations $(6+3k)$, i.e., $(k-3)$.

Adding the three variables c_0, c_1, c_2, brings the total number of yet undetermined variables to k. The number of equations derived from the constraints on $p_3(t)$ is also k. This concludes that if k is equal or greater than three, the number of equations equals the number of variables, and thus, finite number of solutions to the problem may exist.

Let's take a close look on one intermediate segment in $t \in [t_1, t_k]$ (i.e. any segment except for the first one or the last one). $p_3(t)$ is a second-order polynomial, with roots on t_i, t_{i+1}. If $p_3(t)$ is negative, its second-derivative is positive, which leads to the following result:

$$p_3(t) < 0$$
$$\Downarrow$$
$$\tfrac{1}{2}\left(c_0 + \operatorname{sgn}\left(p_3(t)\right)\cdot u_{m2}\right) > 0$$
$$c_0 - u_{m2} > 0$$
$$u_{m2} < c_0$$

If $p_3(t)$ is negative, its second-derivative is positive, and hence

$$p_3(t) > 0$$
$$\Downarrow$$
$$\tfrac{1}{2}\left(c_0 + \operatorname{sgn}\left(p_3(t)\right)\cdot u_{m1}\right) < 0$$
$$c_0 + u_{m1} < 0$$
$$-u_{m1} > c_0$$

Since we assume that none of the segments contain singular trajectories, any two adjacent internal segments must have an opposite sign of $p_3(t)$. This imposes that $u_{m2} < c_0$ and $u_{m1} < -c_0$, which means that either $u_{m1} < 0$ or $u_{m2} < 0$, but u_{m1}, u_{m2} are both positive by definition. The only way which avoids the contradiction is when all the internal nonsingular trajectories are with the same sign, and singular trajectories separate them. This eliminates the possibility of a solution with no singular trajectory segment.

QED (End of proof of Lemma 2.2)

Appendix C

In this appendix we prove lemma 2.3, i.e., we show that the optimal trajectory contains only two switches.

In appendix B we have seen that the optimal trajectory must contain at least one singular trajectory.

In a singular trajectory $p_3(t)=0$ along a segment. This yields that all of its derivatives in the segment become zero, which results in

$$\ddot{p}_3(t) = -\dddot{x} - \dot{p}_2(t) = -\dddot{x} + p_1(t) = -\dddot{x} + c_0 = 0$$
$$\dddot{x}(t) = c_0$$

hence the control signal, $u(t)=\dddot{x}(t)$, has constant values along segments in the time interval, and its form is of switching between these constant values. This implies also that $p_3(t)$ switches between second-order polynomials.

Integrating three times gives the form of $x(t)$ in a singular trajectory:

$$x(t) = \tfrac{1}{6}c_0 t^3 - \tfrac{1}{2}c_1 t^2 + c_2 t + {}^i c_3$$

In a presence of singular trajectories, the continuity constraints are as follows:

$$x(0)=0 \quad x(T)=L \quad x(t_i^-)=x(t_i^+)$$
$$\dot{x}(0)=0 \quad \dot{x}(T)=0 \quad \dot{x}(t_i^-)=\dot{x}(t_i^+)$$
$$\ddot{x}(0)=0 \quad \ddot{x}(T)=0 \quad \ddot{x}(t_i^-)=\ddot{x}(t_i^+)$$

This yields 6+3*k* equations, where *k* is the number of switches, but there are less variables, since c_0, c_1, c_2 are the same in all the singular trajectories. The variables are:

$${}^i d_0, {}^i d_1, {}^i d_2 \qquad i=0..k \;\; \textit{and segment } i \textit{ is not a singular one}$$
$$c_0, c_1, c_2, {}^i c_3 \qquad i=0..k \;\; \textit{and segment } i \textit{ is a singular one}$$
$$t_i \qquad i=1..k$$

The number of parameters to be determined is 4*k* - 2*m* + 6, where *m* is the number of singular trajectories. Here the lower boundary of number of switches is defined by:

$$6+3k \le 4k-2m+6$$
$$k \ge 2m$$

From the above inequality, one can see that the number of switches has to be equal or greater than two (since $m \ge 1$), and the number of segments must be equal or greater than three.

Now assume (by contradiction) that there are more than three segments. If so, there exists at least one internal non-singular trajectory. If $p_3(t)$ is negative in that segment, then,

$$p_3(t) < 0$$
$$\Downarrow$$
$$\tfrac{1}{2}\left(c_0 + \operatorname{sgn}\left(p_3(t)\right)\cdot u_{m2}\right) > 0$$
$$c_0 - u_{m2} > 0$$
$$u_{m2} < c_0$$

Since c_0 is the third derivative of *x*(*t*) in the singular trajectory, this contradicts the control problem definition which bounds the jerk by u_{m_2}.

If $p_3(t)$ is positive in that segment, then,

$$p_3(t) > 0$$
$$\Downarrow$$
$$\tfrac{1}{2}\left(c_0 + \operatorname{sgn}\left(p_3(t)\right)\cdot u_{m1}\right) < 0$$
$$c_0 + u_{m1} < 0$$
$$-u_{m1} > c_0$$

but this contradicts the lower bound of the jerk in the control problem definition. This implies that no nonsingular trajectories can be present in an internal segment, and as a consequence the number of switches is two.

QED (End of proof of Lemma 2.3)

Appendix D

In this appendix we provide the system equations and the boundary and continuity constraints equations in details.

In appendix C we conclude that the trajectory consist of three segments. This yields two switch times in which continuity constraints on the displacement, velocity and acceleration should be satisfied.

The control signal in the first and last segments can be u_{m_2} or $-u_{m_1}$, so there are four possibilities. In order to find the solution(s) we have to solve four equation systems. Only solutions with switching times in the interval $t \in [0,T]$ can be accepted. It is not difficult to find out that the only system that gives an acceptable solution is the one with positive control signal in the first and last segments.

The continuity constraints on displacement are:

$$\tfrac{1}{6}u_{m_2}t_1^{\,3} + \tfrac{1}{2}\,{}^0d_0t_1^{\,2} + {}^0d_1t_1 + {}^0d_2 = \tfrac{1}{6}c_0t_1^{\,3} + \tfrac{1}{2}c_1t_1^{\,2} + c_2t_1 + c_3$$

$$\tfrac{1}{6}c_0t_2^{\,3} + \tfrac{1}{2}c_1t_2^{\,2} + c_2t_2 + c_3 = \tfrac{1}{6}u_{m_2}t_2^{\,3} + \tfrac{1}{2}\,{}^2d_0t_2^{\,2} + {}^2d_1t_2 + {}^2d_2$$

the continuity constraints on velocity are:

$$\tfrac{1}{2}u_{m_2}t_1^{\,2} + {}^0d_0t_1 + {}^0d_1 = \tfrac{1}{2}c_0t_1^{\,2} + c_1t_1 + c_2$$

$$\tfrac{1}{2}c_0t_2^{\,2} + c_1t_2 + c_2 = \tfrac{1}{2}u_{m_2}t_2^{\,2} + {}^2d_0t_2 + {}^2d_1$$

and the continuity constraints on acceleration are:

$$u_{m_2}t_1 + {}^0d_0 = c_0t_1^{\,2} + c_1$$

$$c_0t_2 + c_1 = u_{m_2}t_2 + {}^2d_0$$

In addition, the boundary conditions should also be satisfied.

$$x(0) = 0 \quad x(T) = L$$

$$\dot{x}(0) = 0 \quad \dot{x}(T) = 0$$

$$\ddot{x}(0) = 0 \quad \ddot{x}(T) = 0$$

where u_{m_1}, u_{m_2}, L, T are part of the problem definition, and ${}^0d_0, {}^0d_1, {}^0d_2, c_0, c_1, c_2, c_3, {}^2d_0, {}^2d_1, {}^2d_2, t_1, t_2$ are the unknown parameters.

A system with twelve equations and twelve unknown parameters is obtained.

Solving this system yields the following results:

$$t_1 = \frac{T}{2}\left(1 - \sqrt{\frac{u_{m_2} \cdot T^3 - 24 \cdot L}{u_{m_2} \cdot T^3}}\right) \quad ; \quad t_2 = \frac{T}{2}\left(1 + \sqrt{\frac{u_{m_2} \cdot T^3 - 24 \cdot L}{u_{m_2} \cdot T^3}}\right)$$

$$c_0 = \frac{-24 u_{m_2} \cdot L}{u_{m_2} \cdot T^3 - 24 \cdot L + \sqrt{u_{m_2} \cdot T^3 \left(u_{m_2} \cdot T^3 - 24 \cdot L\right)}}$$

$$c_1 = \frac{-12 u_{m_2} \cdot L \cdot T}{u_{m_2} \cdot T^3 - 24 \cdot L + \sqrt{u_{m_2} \cdot T^3 \left(u_{m_2} \cdot T^3 - 24 \cdot L\right)}}$$

$$c_2 = \frac{\left(12 \cdot L - u_{m_2} \cdot T^3\right)\sqrt{u_{m_2} \cdot T} + u_{m_2} \cdot T^2 \sqrt{u_{m_2} \cdot T^3 - 24 \cdot L}}{4\sqrt{u_{m_2} \cdot T^3 - 24 \cdot L}}$$

$$c_3 = \frac{\left(6 \cdot L - u_{m_2} \cdot T^3\right)\sqrt{u_{m_2} \cdot T^3 - 24 \cdot L} + \left(u_{m_2} \cdot T^3 - 18 \cdot L\right)\sqrt{u_{m_2} \cdot T^3}}{12\sqrt{u_{m_2} \cdot T^3 - 24 \cdot L}}$$

$${}^0d_0 = {}^0d_1 = {}^0d_2 = 0$$

$${}^2d_0 = -u_{m_2} \cdot T \quad ; \quad {}^2d_1 = \frac{u_{m_2} \cdot T^2}{2} \quad ; \quad {}^2d_2 = L - \frac{u_{m_2} \cdot T^3}{6}$$

References

Abend W., Bizzi E., Morasso P. (1982) Human arm trajectory formation. Brain 105: 331-348

Barto A.G., Fagg A.H., Sitkoff N., Houk J.C. (1999) A cerebellar model of timing and prediction in the control of reaching. Neural Computation 11: 565-594

Bernstein N. (1967) The Coordination and Regulation of Movements. Pergamon Press, Oxford

Bhushan N., Shadmehr R. (1999) Computational nature of human adaptive control during learning of reaching movements in force fields. Bilological Cybernetics 81: 39-60

Dingwell J.B., Mah C.D., Mussa-Ivaldi FA (2004) Experimentally confirmed mathematical model for human control of a non-rigid object. Journal of Neurophysiology 91: 1158-1170

Doeringer J.A., Hogan N. (1998) Intermittency in preplanned elbow movements persists in the absence of visual feedback. Journal of Neurophysiology 80: 1787-1799

Fishbach A., Roy S.A., Bastianen C, Miller LE, Houk JC (2005) Kinematic properties of on-line error corrections in the monkey. Experimental Brain Research 164: 442-457

Flash T., Hogan N. (1985) The coordination of arm movements: An experimentally confirmed mathematical model. Journal of Neuroscience 5: 1688-1703

Flash T., Sejnowski T.J. (2001) Computational approaches to motor control. Current Opinion in Neurobiology 11: 655-662

Gomi H., Kawato M. (1996) Equilibrium-point control hypothesis examined by measured arm stiffness during multijoint movement. Science 272: 117-120

Gribble P.L., Ostry D.J., Sanguineti V., Laboissiere R. (1998) Are complex control signals required for human arm movement? Journal of Neurophysiology 79: 1409-1424

Hanneton S., Berthoz A., Droulez J., Slotine J.J.E. (1997) Does the brain use sliding variables for the control of movements? Biological Cybernetics 77: 381-393

Harris C.M., Wolpert D.M. (1998) Signal-dependent noise determines motor planning. Nature 394: 780-784

Hogan N. (1984) An Organizing Principle for a Class of Voluntary Movements. Journal of Neuroscience 4: 2745-2754

Jordan M.I. (1996) Computational aspects of motor control and motor learning. In: Heuer H., Keele S. (eds) Handbook of Perception and Action: Motor Skills. Academic Press, New York

Karniel A., Inbar G.F. (1997) A model for learning human reaching movements. Biological Cybernetics 77: 173-183

Karniel A., Inbar G.F. (1999) The use of a nonlinear muscle model in explaining the relationship between duration, amplitude, and peak velocity of human rapid movements. Journal of Motor Behavior 31: 203-206

Karniel A., Mussa-Ivaldi F.A. (2002) Does the motor control system use multiple models and context switching to cope with a variable environment? Experimental Brain Research 143: 520-524

Karniel A., Mussa-Ivaldi F.A. (2003) Sequence, time, or state representation: how does the motor control system adapt to variable environments? Biological Cybernetics 89: 10-21

Karniel A., Mussa-Ivaldi F.A., d'Avella A., Bizzi E. (2002) A minimum transition hypothesis to account for motor synergies. In: The twelve annual neural control of movement meeting, Naples, Florida

Kashima T., Isurugi Y. (1998) Trajectory formation based on physiological characteristics of skeletal muscles. Biological Cybernetics 78: 413-422

Kirk D.E. (1970) Optimal control theory: An Introduction. Prentice-Hall, New Jersey

Krylow A.M., Rymer W.Z. (1997) Role of intrinsic muscle properties in producing smooth movements. IEEE Transactions on Biomedical Engineering 44: 165-176

Lewis F.L. (1992) Applied optimal control & estimation. Prentice Hall, New Jersey

Loewenstein Y., Mahon S., Chadderton P., Kitamura K., Sompolinsky H., Yarom Y., Hausser M.H. (2005) Bistability of cerebellar Purkinje cells modulated by sensory stimulation. Nature Neuroscience 8: 202-211

Macki J., Strauss A. (1982) Introduction to optimal control theory. Springer-Verlag, New York

Morasso P. (1981) Spatial control of arm movements. Experimental Brain Research 42: 223-227

Mussa-Ivaldi F.A., Bizzi E. (2000) Motor learning through the combination of primitives. Philosophical Transactions of the Royal Society of London Series B-Biological Sciences 355: 1755-1769

Nelson W.L. (1983) Physical Principles for Economies of Skilled Movements. Biological Cybernetics 46: 135-147

Novak K.E., Miller L.E., Houk J.C. (2002) The use of overlapping submovements in the control of rapid hand movements. Experimental Brain Research 144: 351-364

Patton J.L., Mussa-Ivaldi F.A. (2004) Robot-assisted adaptive training: Custom force fields for teaching movement patterns. Ieee Transactions on Biomedical Engineering 51: 636-646

Pontryagin L.S., Boltyanskii V., Gamkrelidze R., Mishchenko, E. (1962) The Mathematical Theory of Optimal Processes. John Wiley & Sons

Richardson M.J.E., Flash T. (2002) Comparing smooth arm movements with the two-thirds power law and the related segmented-control hypothesis. Journal of Neuroscience 22: 8201-8211

Shadmehr R., Mussa-Ivaldi F.A. (1994) Adaptive representation of dynamics during learning of a motor task. Journal of Neuroscience 14: 3208-3224

Shadmehr R., Wise S.P. (2005) The Computational Neurobiology of Reaching and Pointing: A Foundation for Motor Learning. MIT Press

Smith M.A., Brandt J., Shadmehr R. (2000) Motor disorder in Huntington's disease begins as a dysfunction in error feedback control. Nature 403: 544-549

Sosnik R., Hauptmann B., Karni A., Flash T. (2004) When practice leads to co-articulation: the evolution of geometrically defined movement primitives. Experimental Brain Research 156: 422-438

Stein R.B., Oguztoreli M.N., Capaday C. (1986) What is optimized in muscular movements? In: Jones NL MN, McComas AJ (ed) Human Muscle Power. Human Kinetics, Champaign, IL, pp 131-150

Svinin M., Goncharenko I., Zhi-Wei L., Hosoe S. (2006) Reaching movements in dynamic environments: how do we move flexible objects? IEEE Transactions on Robotics and Automation 22: 724-739

Uno Y., Kawato M., Suzuki R. (1989) Formation and Control of Optimal Trajectory in Human Multijoint Arm Movement - Minimum Torque-Change Model. Biological Cybernetics 61: 89-101